

## Relation between carbon isotopes of plants and soils on Marajó Island, a large tropical island: Implications for interpretation of modern and past vegetation dynamics in the Amazon region

M.I. Francisquini<sup>a</sup>, C.M. Lima<sup>a</sup>, L.C.R. Pessenda<sup>a,\*</sup>, D.F. Rossetti<sup>b</sup>, M.C. França<sup>c</sup>, M.C.L. Cohen<sup>d</sup>

<sup>a</sup> Universidade de São Paulo, Laboratório <sup>14</sup>C, Avenida Centenário 303, 13416000 Piracicaba, SP, Brazil

<sup>b</sup> Instituto Nacional de Pesquisas Espaciais-INPE, Rua dos Astronautas 1758-CP 515, 12245-970 São José dos Campos, SP, Brazil

<sup>c</sup> Federal Institute of Pará, Av. Almirante Barroso 1155, Marco, CEP: 66090-000 Belém, PA, Brazil

<sup>d</sup> Federal University of Pará, Av. Perimetal 2651, Terra Firme, CEP: 66077-530 Belém, PA, Brazil

### ARTICLE INFO

#### Article history:

Received 26 June 2013

Received in revised form 25 February 2014

Accepted 6 March 2014

Available online 31 March 2014

#### Keywords:

Paleovegetation  
Modern vegetation  
Soil  
Carbon isotopes  
Marajó Island

### ABSTRACT

We assess the relation between the contrasting vegetation types of rainforest, open savanna and wooded savanna coexisting in close contact on Marajó Island at the mouth of the Amazon River. Floristic and carbon isotopic characterizations of modern plants were combined with organic matter carbon isotope and grain size records of soil to characterize vegetation evolution at six locations on southeastern and northeastern Marajó Island and its relations to climate changes since the late Pleistocene. C<sub>3</sub> plants contribute 100% of the biomass in the rainforest on post-Barreiras sediments (site 1). No significant vegetation changes are evident in these places since at least ~7860 cal yr B.P. Rainforests on paleochannels (sites 4 and 6) are protected from flooding by slightly elevated sandy levee and have flora very similar to site 1. These forests were formed since the early-mid Holocene after channel abandonment. C<sub>3</sub> grasses are predominant in open savanna areas (sites 4, 5 and 6), with less representation in wooded savannas (sites 2 and 3). However, C<sub>4</sub> grasses, despite having fewer species, constitute significant biomass in the wooded (~60%) and open savanna vegetation areas, especially during the dry season. The reconstructions of past vegetation together with the distributions of modern vegetation allow prediction that climate changes to drier conditions can significantly influence the future Marajó Island landscape, likely enabling expansion of C<sub>4</sub> plants in the flooding zone and of trees in the rainforests.

© 2014 Elsevier B.V. All rights reserved.

### 1. Introduction

The evolution of the modern Amazon landscape and its flora has been particularly influenced by late Pleistocene and Holocene climate changes (Sifeddine et al., 1994; Gouveia et al., 1997; Turcq et al., 1998; Freitas et al., 2001; Pessenda et al., 2001; Sifeddine et al., 2001; Ledru et al., 2006, 2007; Lima, 2008; Cordeiro et al., 2011), tectonic events (Rossetti and Valeriano, 2007; Miranda et al., 2009; Rossetti, 2010; Rossetti et al., 2010, 2012), and relative sea level variations (Behling and Costa, 2000; Behling et al., 2001; Cohen et al., 2005a,b). The diversity of these influences could explain the variety of distinct vegetation phytotypes on fluvial Marajó Island, such as dense Amazonian rainforest on western side of the island, vegetation on paleochannels, areas of open savanna that are flooded during the rainy season, and areas of wooded savanna outside of the flooded area (Pires and Prance, 1985).

Open and wooded savanna areas next to predominantly tropical forests have generally received much attention, because both are part of an ecosystem that in the past presented contrasting vegetation structures

and contacts due to climate dynamics and geological events. For instance, the Brazilian savanna expanded and replaced rainforest during dry periods in the late Pleistocene (Ledru et al., 2006) and early to mid Holocene (Absy et al., 1991; Gouveia et al., 1997; Pessenda et al., 1998a,b; Turcq et al., 1998; Carneiro-Filho et al., 2002; Pessenda et al., 2004; Vidotto et al., 2007; Pessenda et al., 2010; Cordeiro et al., 2011), that were accompanied by climate fluctuations (Van der Hammen, 1974; Absy et al., 1991; Desjardins et al., 1996; Pessenda et al., 1998a,b; Behling and Costa, 2000; Freitas et al., 2001; França et al., 2012). In addition, tectonic events (Rossetti et al., 2008b) could also have caused changes in river and tributary flow discharge (Cohen et al., 2012) and influenced paleoestuary activation through the Pleistocene–Holocene (Rossetti et al., 2008a,b), all of which further influenced local vegetation.

Floristic and isotopic characterizations of modern plants of contrasting vegetation types coexisting in close contact provide useful insights to help understand the modern Amazon vegetation distribution on Marajó Island. Carbon isotope records help to distinguish organic matter contributions from C<sub>3</sub> (trees, shrubs and some grasses) and C<sub>4</sub> (grasses) plants. In general, C<sub>3</sub> and C<sub>4</sub> land plants show  $\delta^{13}\text{C}$  values between  $-33\text{‰}$  and  $-20\text{‰}$ , and  $-15\text{‰}$  and  $-9\text{‰}$ , respectively (Deines, 1980). Grain size measurements and radiocarbon dating allow understanding the

\* Corresponding author. Fax: +55 19 3429 4656.  
E-mail address: [pessenda@cena.usp.br](mailto:pessenda@cena.usp.br) (L.C.R. Pessenda).

evolution and consolidation of paleochannels and the open savanna areas on flooded zones.

The goal of this paper is to characterize the dominant species and respective carbon isotopic values of different vegetation phytotypes in order to understand modern plant dynamics on the Marajó Island landscape, northern Amazon region, and to reconstruct the late Pleistocene–Holocene vegetation changes, focusing on the carbon isotopic relation between the ancient and modern soil organic matter of the region.

## 2. Study area

Marajó Island is the main island of the Marajó Archipelago on the Pará and Amapá coast of northern Brazil and at the mouth of the Amazon River. It constitutes 400,100 km<sup>2</sup> of the area of the archipelago, and the smaller neighboring islands that are separated from it by rivers constitute the remaining 90,000 km<sup>2</sup> of area. The entire archipelago has a fluvial-marine setting, being surrounded by the Pará River to the south, the Tocantins River–Marajó Bay to the east, the Atlantic Ocean to the north, and the Amazon River mouth to the west. Land elevation on the western side of the island is on average 20 m and reaches as high as 42 m, and it is between 2 and 6 m with a mean of 4 m on the eastern side (Fig. 1). The dominant vegetation is a dense rainforest on oxisols (Soil Survey Staff, 1999).

Climate is warm and wet tropical, with a mean annual temperature of 27 °C and mean annual precipitation of approximately 3000 mm (IDESP, 1974). Wet and dry periods are well defined, with the rainy season occurring between January and July (Bezerra et al., 1990), when open savanna areas from eastern Marajó Island become completely flooded (Rossetti et al., 2010). A low precipitation period (dry season) occurs between August and December (Bezerra et al., 1990).

Many small channels, straight or meandering, permanent or ephemeral, and interspersed ponds make up the hydrological system (Bemerguy, 1981). The discharge of the nearby Amazon River averages about 170,000 m<sup>3</sup> s<sup>-1</sup>, with maximum and minimum outflow of 270,000 m<sup>3</sup> s<sup>-1</sup> in the wet season and 60,000 m<sup>3</sup> s<sup>-1</sup> in the dry season (ANA, 2003).

In the eastern flooded environment, a few levees that are covered by fine sand and silt are slightly elevated above water level, and are favorable for tree growth. Known as paleochannels, these areas are results of abandonment of numerous channels that were filled but are still evident in the landscape (Projeto Radam, 1974).

On paleochannel boundaries, flat and slightly low-lying floodplains in the open savanna are covered by grasses and other herbaceous plants, especially by two species, *Ipomea asarifolia* and *Ipomea carnea*, and also in some places with arboreal and shrub species in grassy areas. The soils are classified as gleysols and vertisols according to USDA soil taxonomy (Soil Survey Staff, 1999).

The Miocene deposits of the Barreiras Formation that occur from northern to southeastern Brazil (Arai, 2006) must be found at most elevated surface at eastern Marajó Island side and is covered mainly by post-Barreiras deposits (Fig. 1) of Pleistocene and Holocene age (Rossetti et al., 2012). The Marajó Island Quaternary history is postulated to have been tightly controlled by tectonic events that led to subsidence and creation of new sites to accommodate sediment (Rossetti et al., 2008b, 2012). Thus, tectonic subsidence might be responsible for estuarine basin formation (Miranda et al., 2009; Castro et al., 2010), the flooded areas, and the abandonment of the paleo-Tocantins River, leaving numerous paleochannels (Rossetti and Valeriano, 2007; Rossetti et al., 2008a, 2010, 2012).

It is common to find outside of the flooding area wooded savanna (Cerrado vegetation) with distorted trees growing over a soil consisting

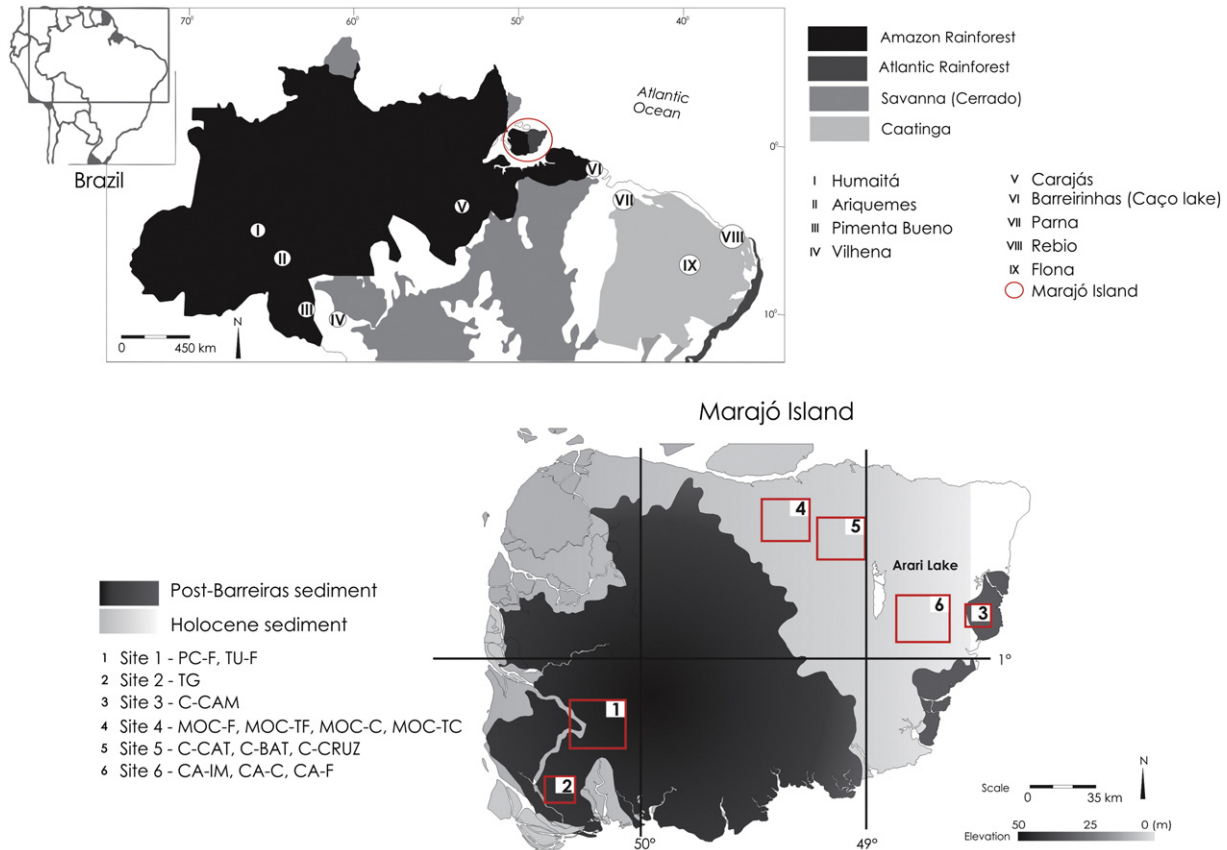


Fig. 1. Map showing the relative position of Brazilian biomes (Rainforest, Cerrado, Caatinga and Atlantic Rainforest) highlighting some studies in latitude between 0° and 10°S (edited from Pessenda et al., 2010), the Marajó Island and respective sampling sites.

of kaolinitic material and mottled with a concretionary lateritic level at 1.40 meter subsurface, indicating an aluminum enriched soil that is classified as plinthosols according to USDA (Soil Survey Staff, 1999).

### 3. Sampling and methods

Soil samples were collected at 10 cm intervals during the dry season in trenches and by drillings up to 400 cm depth at fourteen locations on the southwestern and northeastern parts of the island (Fig. 2A, B and Table 1). The fourteen sampling points were grouped into six sites to facilitate visualization and interpretation of the results. Site 1 (PC-F, TU-F) is located in rainforest, site 2 (TG) (Fig. 2A) and site 3 (C-CAM)

(Fig. 2B) are located in wooded savanna vegetation. These sites are outside of the flooding zone on post-Barreiras Formation terrain (Rossetti et al., 2010) and are considered as reference locations for soil organic carbon isotope analyses that can provide information about past vegetation dynamics and possible climate inferences. Site 4 (MOC-F, MOC-TF, MOC-C, MOC-TC) represents forested areas on paleochannels (MOC-F and MOC-TF) and open savanna (MOC-C and MOC-TC) in close contact between the transition rainforest and flooding zone. Site 5 (C-CAT, C-BAT, C-CRUZ) is an open savanna area near Arari Lake in the flooding zone, and site 6 (CA-C, CA-F, CA-IM) is nearest to the eastern coast of the flooding zone and represents a transitional forest on a paleochannel (CA-IM) – open savanna (CA-C) – forest on a paleochannel (CA-F) setting.

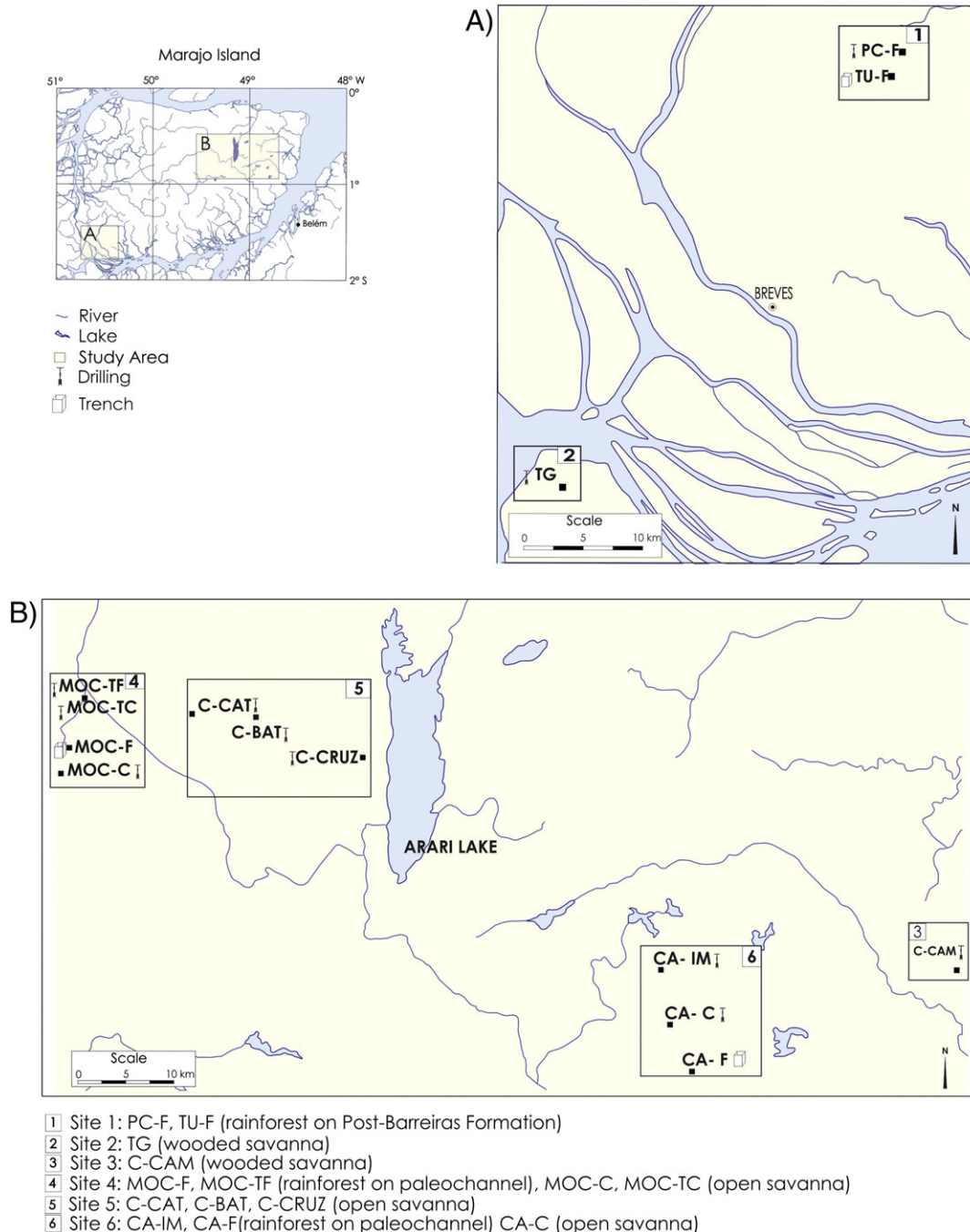


**Fig. 2.** Marajo Island map emphasizing two collect areas, (A) at Southeastern and (B) at Northeastern. Sites are also described: at area A – site 1 (PC-F, TU-F) and site 2 (TG); at area B – site 3 (C-CAM), site 4 (MOC-C, MOC-TC, MOC-F, MOC-TF), site 5 (C-CAT, C-BAT, C-CRUZ) and site 6 (CA-IM, CA-C, CA-F).

**Table 1**  
Latitudinal and longitudinal localization of sampling points, containing vegetation type's classification, sampling method and sample depth (cm).

	Collect point	Vegetation	Latitude	Longitude	Sampling	Depth (cm)
Site 1	TU-F	Forest	1°30.349' S	50°23.006' W	Trench	230
	PC-F	Forest	1°29.028' S	50°22.902' W	Drilling	390
Site 2	TG	Wooded savanna	1°50.145' S	50°38.684' W	Drilling	270
Site 3	C-CAM	Wooded savanna	0°52.137' S	48°37.754' W	Drilling	140
Site 4	MOC-F	Forest	0°38.824' S	49°27.926' W	Trench	310
	MOC-C	Open savanna	0°39.972' S	49°28.065' W	Drilling	370
	MOC-TC	Open savanna	0°35.875' S	49°26.692' W	Drilling	210
	MOC-TF	Forest	0°35.868' S	49°26.692' W	Drilling	330
Site 5	C-CAT	Open savanna	0°36.773' S	49°20.699' W	Drilling	210
	C-CRUZ	Open savanna	0°39.399' S	49°11.101' W	Drilling	310
	C-BAT	Open savanna	0°36.830' S	49°16.965' W	Drilling	400
Site 6	CA-IM	Forest	0°51.994' S	48°54.469' W	Drilling	360
	CA-C	Open Savanna	0°54.861' S	48°54.425' W	Drilling	210
	CA-F	Forest	0°58.227' S	48°52.850' W	Trench	330

The floristic survey consisted of a brief ecological evaluation to record the vegetation pattern distributions. Descriptions were made by inventorying all vascular plant species in a radius of approximately 20 m from each sampling point and registering species occurrences as: (1) abundant, more representative populations; (2) common, numerous but not so expressive and (3) rare, random or atypical species.

Soil samples were systematically taken each 10 cm for analyses and described according to their color changes (Munsell, 2009), grain size and texture. Grain size distributions used 120 g of soil *in natura* with analyses carried out according to densimeter standard procedures (Kiehl, 1979) at the Soil Department of ESALQ/USP. The results are expressed in percentages of the sand (2–0.0625 mm), silt (62.5–3.9 µm), and clay (3.9–0.12 µm) fractions.

Carbon isotope ( $\delta^{13}\text{C}$ ) analyses of soil organic matter were performed at all fourteen sampling points from the base to the shallow layer (0–10 cm) of the profiles and on modern dominant plant species collected around each point. After physical pretreatment that constituted of removal of insects and rootlets by hand-picking and floatation (Pessenda et al., 1996b), samples of ~70 mg were analyzed at the Stable Isotope Laboratory of CENA/USP (São Paulo, Brazil) on an elementary analyzer attached to a Scientific Europa ANCA-SL 20/20 mass spectrometer. Total organic carbon (TOC) results are expressed as percentage of dry weight of soil or plant tissue with an analytical precision of 0.09%, and  $\delta^{13}\text{C}$  values are given with respect to VPDB (Vienna Pee Dee Belemnite Standard) with an analytical precision of  $\pm 0.2\%$ .

Vegetation changes recorded in soils are related to proportions of carbon derived from  $\text{C}_3$  and  $\text{C}_4$  sources and its mixture, which can be estimated by the carbon-isotope mass balance equation (Boutton et al., 1998):

$$\delta^{13}\text{C}(\text{‰}) = (\delta^{13}\text{C}_{\text{C}_4})(x) + (\delta^{13}\text{C}_{\text{C}_3})(1-x),$$

where  $\delta^{13}\text{C}$  if for the whole soil sample,  $\delta^{13}\text{C}_{\text{C}_4}$  and  $\delta^{13}\text{C}_{\text{C}_3}$  are the average  $\delta^{13}\text{C}$  values of the  $\text{C}_4$  (–13‰) and  $\text{C}_3$  (–27‰) plant endmembers,  $x$  is the proportion of carbon from  $\text{C}_4$  plants, and  $1 - x$  is the proportion of carbon derived from  $\text{C}_3$  plants.

Fifteen pretreated soil and plant fragments with masses  $\geq 1.0$  g were dated by accelerator mass spectrometer (AMS) at Isotrache Laboratory, Toronto (Canada) and at AMS-Labor Erlangen (Germany). Contaminants, such as rootlets, were physically eliminated during the pretreatment. The organic matter (humins) from soil samples was obtained after the pretreatment using an acid–alkali–acid treatment followed by washings with distilled water until pH 6 and drying of the final residue at 50 °C (Pessenda et al., 1996b, 2009). Radiocarbon ages are reported as  $^{14}\text{C}$  yr (1  $\sigma$ ) B.P. (before AD 1950), normalized to a  $\delta^{13}\text{C}$  of –25‰ VPDB and in calibrated years as cal yr (2  $\sigma$ ) B.P. (Reimer et al., 2009). All results

and discussions are based on the mean calibrated age (cal yr B.P.; França et al., 2012; Pessenda et al., 2012; Zani et al., 2012).

In sites 2 (TG) and 3 (C-CAM), radiocarbon dating was not performed because the soil sampling was done only by drilling, which usually does not yield samples suitable for reliable  $^{14}\text{C}$  dating because of interlayer contamination. To obtain reliable and representative  $^{14}\text{C}$  ages of soil organic matter for sampling sites 1, 4 and 6, we selected the locations for the trenches considering tops of small slopes and similarities with respect to vegetation cover, soil lithology, grain size, and degree of flooding. At site 5 (flooding zone) the trenching was not done because of a very shallow water table at this location. Instead, sampling was done here by drilling and looking for buried plant fragments (pretreated dry mass  $\geq 1.0$  g) that were considered more suitable for radiocarbon dating than soil organic matter at this waterlogged location.

## 4. Results and discussion

### 4.1. Radiocarbon dating

Radiocarbon dates obtained from each sampling point and their respective depths are presented in Table 2. The TU-F samples from the rainforest on the western side that also representative for the PC-F samples (site 1), yield dates from ~7859 cal yr B.P. at 160–150 cm to ~3326 cal yr B.P. (70–60 cm). Approximately the same ages are found for the layers 250–240 cm (~7722 cal yr B.P.) and 160–150 cm (~7859 cal yr B.P.). These similar dating results from 250 to 150 cm soil depths probably reflect bioturbation caused by soil fauna (Boulet et al., 1995; Gouveia and Pessenda, 2000) and the small mass and carbon content of the collected sample. Several cases in our studies (Pessenda et al., 1996a,b, 1998b) show that very small samples can contain a high concentration of young or old contaminants coming from shallow or deeper soil horizons, even after the physical and chemical pretreatments. These analytical procedures remove only the adsorbed contaminants, whereas materials absorbed in the past during the sample deposition can remain in the residual organic matter (humins fraction) and contribute significantly to the final (younger/older) artificial age.

Age inversions were observed for the MOC-F samples that are also representative for the MOC-TF samples from the paleochannel outside of the flooded zone. The humin fraction at 300–290 cm soil depth yields an age of ~19,189 cal yr B.P., whereas two plant fragments collected at 310–300 cm and 250–240 cm are dated at ~9640 cal yr. B.P. and ~8910 cal yr B.P., respectively. Despite the mass of at least ~1 g of these plant fragments, the inversions may result from transport by soil water percolation, water table dynamics, and bioturbation processes that contribute to the burial of wood and charcoal fragments and for distinct soil formation rates (Boulet et al.,

**Table 2**

Radiocarbon dating reported as <sup>14</sup>C yr (1 σ) B.P., normalized to calibrated years as cal yr (2 σ) B.P. (Reimer et al., 2009) and mean calibrated age (cal yr B.P.) of humin fraction and vegetal fragment samples.

	Sample	Depth (m)	Laboratory number	Material	Age ( <sup>14</sup> C yr B.P.)	Age (cal yr B.P., 2 σ)	Mean calibrated age (cal yr B.P.),
Site 1	TU-F	70–60	Erl <sup>a</sup> 10804	Vegetal fragment	3117 ± 34	3271–3382	~3326
	TU-F	100–90	TO <sup>b</sup> 13480	Humin	4390 ± 80	4839–5287	~5063
	TU-F	160–150	Erl <sup>a</sup> 13481	Humin	7000 ± 80	7755–7963	~7859
	TU-F	250–240	TO <sup>b</sup> 13482	Humin	6850 ± 100	7515–7929	~7722
Site 4	MOC-F	100–90	Erl <sup>a</sup> 10796	Humin	8464 ± 38	9438–9531	~9438
	MOC-F	200–190	Erl <sup>a</sup> 10797	Humin	10,387 ± 38	12,087–12,410	~12,248
	MOC-F	250–240	Erl <sup>a</sup> 10798	Vegetal fragment	8048 ± 36	8774–9029	~8901
	MOC-F	300–290	Erl <sup>a</sup> 10799	Humin	16,118 ± 60	18,941–19,438	~19,189
Site 5	MOC-F	310–300	Erl <sup>a</sup> 10800	Vegetal fragment	8685 ± 39	9544–9737	~9640
	C-BAT	180–170	Erl <sup>a</sup> 10801	Vegetal fragment	4918 ± 30	5594–5714	~5654
	C-BAT	250–240	Erl <sup>a</sup> 10802	Vegetal fragment	4930 ± 36	5596–5727	~5661
	C-BAT	380–370	Erl <sup>a</sup> 10803	Vegetal fragment	5702 ± 37	6406–6628	~6517
Site 6	C-AF	100–90	TO <sup>b</sup> 13477	Humin	2810 ± 60	2771–3078	~2925
	C-AF	200–190	TO <sup>b</sup> 13478	Humin	5730 ± 80	6320–6718	~6519
	CA-F	320–310	TO <sup>b</sup> 13479	Humin	6330 ± 110	6965–7437	~7201

<sup>a</sup> AMS-Labor Erlangen (Germany).

<sup>b</sup> Isotracer Laboratory, Toronto (Canada).

1995; Gouveia and Pessenda, 2000). Furthermore, for all study areas, a probable influence of tectonic events in the soil accommodation and in the organic matter dynamics cannot be ignored. For the CA-F samples and also representative for the CA-IM samples in the paleochannels inside of the flooded zone dates range from ~7210 cal yr B.P. (320–310 cm) to ~2925 cal yr B.P. at 100–90 cm. The contrast in the oldest ages observed for the MOC-F samples and the CA-F samples is probably associated with the organic matter dynamics of the non-flooded setting, where the soil formation process has a low rate of ~0.016 cm/year, and the flooded system, where the soil formation/sedimentation rate is ~0.032 cm/year.

The radiocarbon dating for the C-BAT samples from the open savanna in the flooded zone, which is also representative for the MOC-C, MOC-TC, C-CAT, C-CRUZ and CA-C samples, show dates that varied from ~6517 cal yr B.P. (380–370 cm), ~5661 cal yr B.P. at 250–240 cm and ~5654 cal yr B.P. at 180–170 cm.

4.2. Grain size analyses

Comparison of the grain size analysis results of the paleochannel and floodplain locations reveals important differences between their soil formation and sedimentation processes (Fig. 3). Cores from paleochannels (MOC-F, MOC-TF) display sand successions that grade upward into sandy silt from the base until ~150 cm (~19,200 cal yr B.P. to ~10,000 cal yr B.P.), and then have silt and mud alternations recording typical channel filling from 150 cm to full abandonment in the shallow layer (~10,000 cal yr B.P. to modern). Floodplain locations (C-CAT, C-CRUZ) show silt and clay predominance through the whole core (~40 and 60%, respectively).

Paleochannel locations MOC-TF and MOC-F are close to each other and have similar textures. In their sedimentary basal package recording the paleochannel development, sand content decreases, from ~60% until ~20% from 90 cm to the top layer, whereas the silt and clay increases

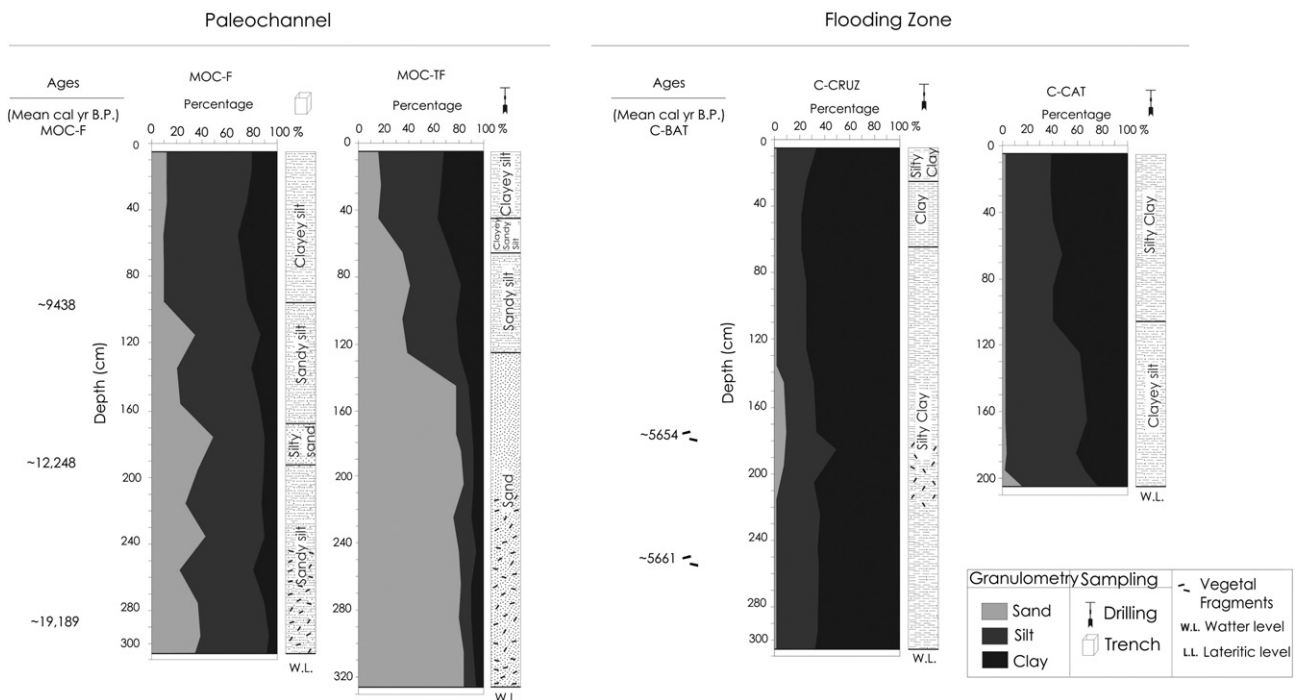


**Fig. 3.** Diagram indicating the relation between sand, silt and clay percentages along the collected core and comparison of paleochannel (MOC-F, MOC-TF and MOC-TC, at site 4) and flooding zone areas (C-CAT and C-CRUZ, at site 5), with respective radiocarbon ages (from MOC-F and C-BAT).

(~40 and 20‰, respectively). MOC-F is comprised essentially of clayey silt material from 100 cm to the top layer. The complete channel abandonment that was followed by sedimentary infilling allowed the surface to be occupied first by grasslands and later by trees. Rossetti et al. (2010) emphasized that slightly higher topographies are responsible for protecting these areas from the effects of flooding and allowing development of rainforests.

#### 4.3. Floristic and isotopic analyses of vegetation

Floristic characterization at the fourteen sampling locations identified a total of 650 species. Relative species richness was recorded for the rainforest on the post-Barreiras Formation, rainforest on paleochannel, open savanna, and wooded savanna. Species from each sampling site are organized according to their representativeness, habitat types (arboreal, shrubby, palms, herbs, and liana), and their respective carbon isotopic values in Figs. 4 to 7.

In the rainforest on the post-Barreiras Formation terrain, plants of site 1 (PC-F and TU-F), have low  $\delta^{13}\text{C}$  values (Fig. 4), ranging between  $-37.8\text{‰}$  (*Ischnosiphon gracilis*) (Maranthaceae) and  $-28.9\text{‰}$  (*Clidemia hirta*) (Melastomataceae). High arboreal density occurs at this sampling point, and the most representative tree species are *Miconia pyriformis* ( $\delta^{13}\text{C} - 34.5\text{‰}$ ) (Melastomataceae) and *Poraqueiba guianensis* ( $\delta^{13}\text{C} - 34.0\text{‰}$ ) (Icacinaceae).  $\text{C}_3$  herb species such as *Clidemia dentata* ( $\delta^{13}\text{C} - 33.7\text{‰}$ ) (Melastomataceae), *Olyra latifolia* ( $\delta^{13}\text{C} - 34.5\text{‰}$ ) (Poaceae), *Selaginella* sp. ( $\delta^{13}\text{C} - 33.2\text{‰}$ ) (Selaginellaceae) and *Ischnosiphon gracilis* (Maranthaceae) ( $\delta^{13}\text{C} - 37.8\text{‰}$ ) are also highly representative. The shallow (0–10 cm layer) soil isotopic  $\delta^{13}\text{C}$  values of  $-28.9\text{‰}$  to PC-F and  $-28.6\text{‰}$  to TU-F indicate rainforest biomass contributions of 100%  $\text{C}_3$  plants to soil organic matter.

Plants at TG, site 2, and C-CAM, site 3, (Fig. 5) include arboreal species typical of central-eastern Brazilian wooded savanna, such as *Tabebuia serratifolia* ( $\delta^{13}\text{C} - 27.3\text{‰}$ ) (Bignoniaceae), *Curatella americana* ( $\delta^{13}\text{C} - 28.9\text{‰}$ ) (Dilleniaceae) and *Pouteria ramiflora* ( $\delta^{13}\text{C} - 28.9\text{‰}$ ) (Sapotaceae), and of north and northeastern Brazilian savanna, such as *Byrsonima crassifolia* ( $\delta^{13}\text{C} - 27.8\text{‰}$ ) (Malpighiaceae) and *Anacardium microcarpum* ( $\delta^{13}\text{C} - 28.9\text{‰}$ ) (Anacardiaceae). Also present are the  $\text{C}_4$  Poaceae species *Axonopus purpusii* ( $\delta^{13}\text{C} - 11.8\text{‰}$ ), *Andropogon selleanus* ( $\delta^{13}\text{C} - 11.8\text{‰}$ ), and *Paspalum pulchellum* ( $\delta^{13}\text{C}$

$-12.4\text{‰}$ ).  $\delta^{13}\text{C}$  values of the total plant assemblage range from  $-11.1\text{‰}$  (*Vigna longifolia*) (Fabaceae) to  $-33.0\text{‰}$  (*Myrcia cúprea*) (Myrtaceae). The shallow soil isotopic values of  $-18.3\text{‰}$  at C-CAM and  $-17.3\text{‰}$  at TG indicate a larger biomass contribution from  $\text{C}_4$  plants than from  $\text{C}_3$  plants at these wooded savanna sites (~63%  $\text{C}_4$  at C-CAM and 69%  $\text{C}_4$  at TG) than at the rainforest site.

Compositions of vegetation at the paleochannel locations MOC-F, MOC-TF (site 4), CA-IM, and C-AF (site 6) are quite similar to that of the rainforest from site 1 (PC-F, TU-F) in both floristic and isotopic values (Fig. 6). Arboreal species that are present at both sites are *Euterpe oleracea* ( $\delta^{13}\text{C} - 32.6\text{‰}$ ) (commonly known as Açai palm), *Inga grandiflora* ( $\delta^{13}\text{C} - 31.4\text{‰}$ ) (Fabaceae), and *Symphonia globulifera* ( $\delta^{13}\text{C} - 31.0\text{‰}$ ) (Clusiaceae). Other species, such as *Gustavia augusta* ( $\delta^{13}\text{C} - 33.8\text{‰}$ ) (Lecythydaceae), *Simaba multiflora* ( $\delta^{13}\text{C} - 29.9\text{‰}$ ) (Simaroubaceae), *Licania apetala* ( $\delta^{13}\text{C} - 31.9\text{‰}$ ) (Chrysobalanaceae), and *Inga nobilis* ( $\delta^{13}\text{C} - 30.8\text{‰}$ ) (Fabaceae), are common to all sampling points on the paleochannel. No visible evidence of  $\text{C}_4$  plants is observed, and all herbs are  $\text{C}_3$  plants, such as *Panicum laxum* ( $\delta^{13}\text{C} - 27.7\text{‰}$ ) (Poaceae) at CA-IM and MOC-TC, *Olyra longifolia* ( $\delta^{13}\text{C} - 32.5\text{‰}$ ) (Poaceae) at CA-F and *Cyperus surinamensis* ( $\delta^{13}\text{C} - 34.2\text{‰}$ ) (Cyperaceae) at MOC-F. The isotopic values of the shallow soil layer are  $-28.1\text{‰}$  at MOC-F,  $-24.6\text{‰}$  at MOC-TF,  $-26.7\text{‰}$  at CA-IM, and  $-26.6\text{‰}$  at CA-F, suggesting the overall predominance of  $\text{C}_3$  plant contributions to the soil organic matter, ranging from 100% at MOC-F to 93% at MOC-TF, 98% at CA-IM, and 97% at CA-F.

At site 4 (MOC-C, MOC-TC), an open savanna vegetation in contact with the flooding zone,  $\text{C}_3$  grasses are widely represented (Fig. 7), although  $\text{C}_4$  grasses like *Paspalum orbiculatum* ( $-12.0\text{‰}$ ) and a Crassulaceae acid metabolism (CAM) species such as *Guzmania lingulata* ( $-15.9\text{‰}$ ) (Bromeliaceae) are present. Although few in species,  $\text{C}_4$  plants seem to have a relatively large total biomass; the shallow soil carbon isotope values are  $-21.7\text{‰}$  to MOC-C and  $-23.9\text{‰}$  to MOC-TC, suggesting  $\text{C}_4$  plant organic matter contributions of ~38% at MOC-C and 22% at MOC-TC. At C-BAT, C-CAT and C-CRUZ (Site 5), open savanna vegetation near Arari lake (a flooding area),  $\text{C}_3$  grasses and shrubs such as *Ipomoea carnea* ( $\delta^{13}\text{C} - 26.6\text{‰}$ ) (Convolvulaceae) and *Mimosa dormiens* ( $\delta^{13}\text{C} - 29.8\text{‰}$ ) (Fabaceae mimosoidae) are dominant, which is probably associated with the moistness of the area that favors establishment of  $\text{C}_3$  herbs/grasses. Herbs such as *Ipomoea*

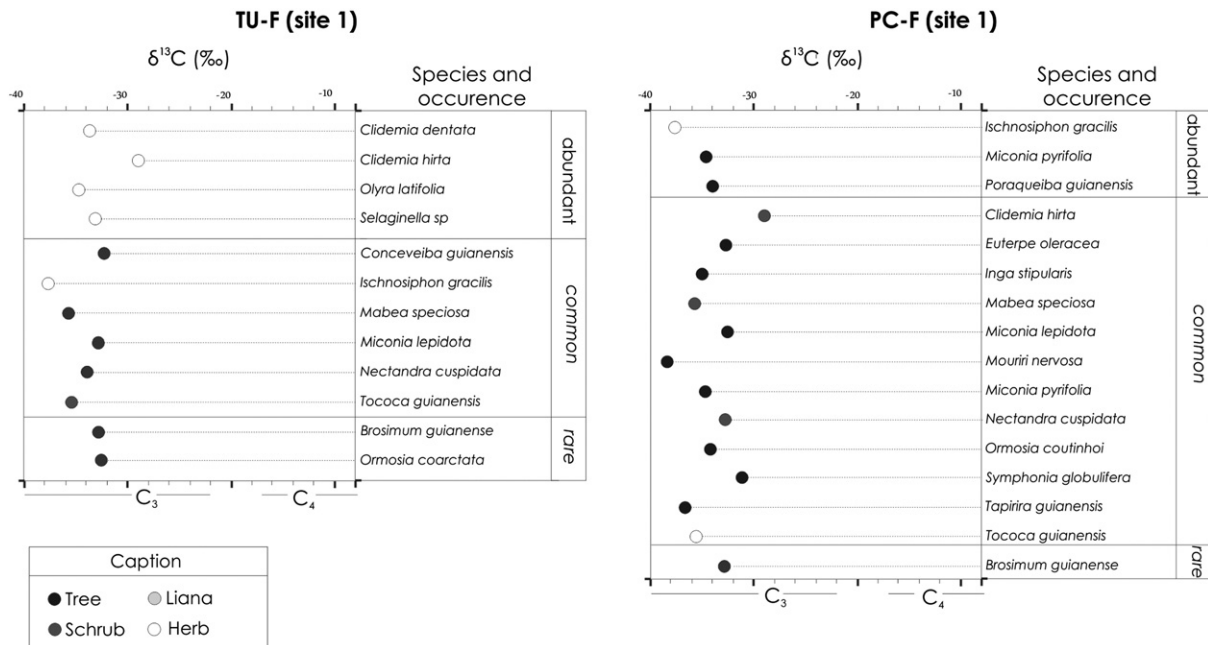


Fig. 4. Plants and their respective isotopic values ( $\delta^{13}\text{C}$ ) of forest on post-Barreiras Formation site 1 (TU-F and PC-F) grouped by their representativeness and vegetation habit (tree, shrub, liana and herbs).

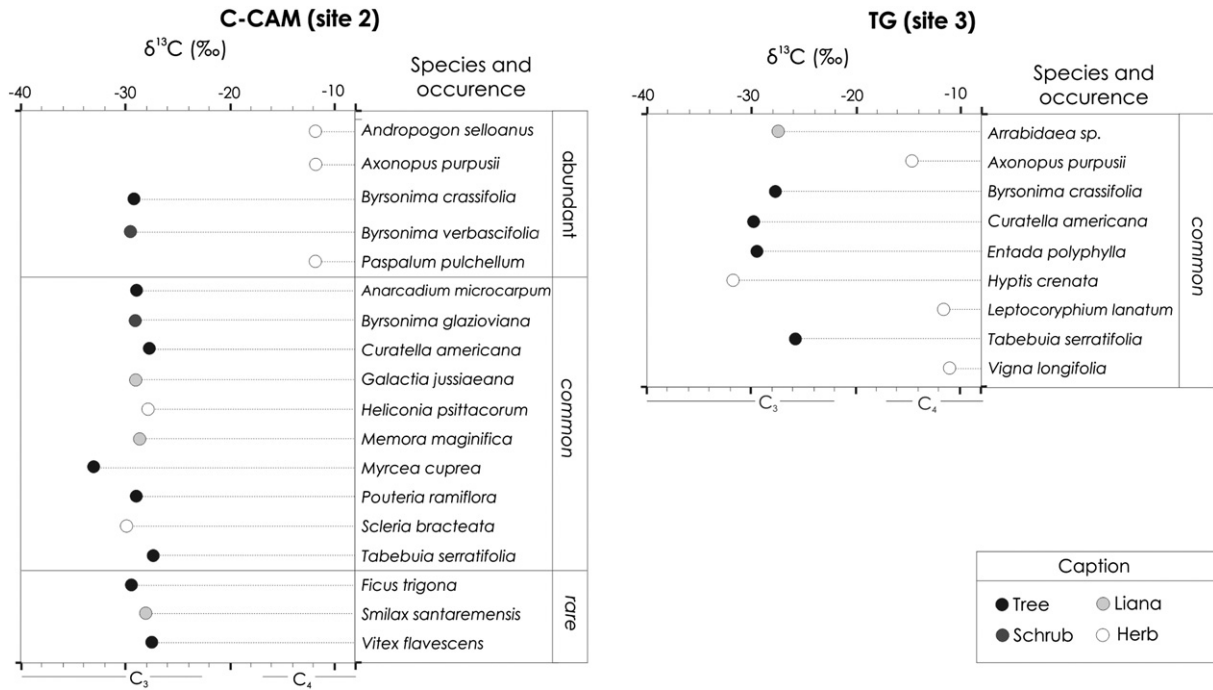


Fig. 5. Plants and their respective isotopic values ( $\delta^{13}\text{C}$ ) of wooded savanna site 2 (TG) and site 3 (C-CAM) grouped by their representativeness and vegetation habit (tree, shrub, liana and herbs).

*asarifolia* ( $\delta^{13}\text{C}$  - 28.9‰) are abundant at the C-BAT and C-CAT locations. In addition,  $\text{C}_4$  Cyperaceae such as *Fimbristylis* sp. ( $\delta^{13}\text{C}$  - 12.4‰), *Bulbostylis truncata* ( $\delta^{13}\text{C}$  - 12.0‰) and  $\text{C}_4$  Poaceae such as *Paspalum orbiculatum* ( $\delta^{13}\text{C}$  - 12.0‰), *Paspalum riparium* ( $\delta^{13}\text{C}$  - 12.1‰) and *Axonopus purpusii* ( $\delta^{13}\text{C}$  - 14.5‰) are also common and are probably associated with the dry season that is favorable for  $\text{C}_4$  plant development. The carbon isotopic values of the shallow soil layer vary fairly narrowly from -19.1‰ at C-CAT, to -20.3‰ at C-CRUZ, and finally -22.2‰ at C-BAT, with  $\text{C}_4$  biomass contributions of ~57%, 47% and 34%, respectively. Although CA-C (Site 6) has only a few  $\text{C}_4$  Poaceae species, such as *Axonopus purpusii* and *Paspalum pulchellum* ( $\delta^{13}\text{C}$  - 12.4‰), the shallow soil isotopic value of -18.7‰ is indicative of ~60%  $\text{C}_4$  biomass contribution to the soil organic matter.

4.4. Stable carbon isotopes ( $\delta^{13}\text{C}$ ) of soil organic matter depth profiles

For interpretation of the soil organic matter  $\delta^{13}\text{C}$  profiles, it was assumed that variations smaller than 3.0‰ are associated with isotopic fractionation occurring during organic matter decomposition and with variations in the carbon isotope composition of atmospheric  $\text{CO}_2$  (Boutton, 1996). Thus, variations of at least 3.0‰ likely resulted from changes in the local plant community (Boutton, 1996; Desjardins et al., 1996; Pessenda et al., 1996a,b, 1998a,b; Freitas et al., 2001; Pessenda et al., 2001; Gouveia et al., 2002; Pessenda et al., 2004, 2005, 2010).

The organic matter  $\delta^{13}\text{C}$  values from each site, as well as the respective calibrated ages with soil depth, are shown in Fig. 8. Samples from the rainforest location TU-F of site 1 exhibit  $\delta^{13}\text{C}$  values varying between -27.9‰ and -27.1‰ (mean of -27.5‰) from 250 to 170 cm (~7859 cal yr B.P.), which are values that also characterize the modern forest vegetation cover. A slight  $\delta^{13}\text{C}$  increase from ~-26.8‰ to ~-25.9‰ (mean of -26.2‰) occurs between 170 and 60 cm, an interval that corresponds to ~7859 cal yr B.P. to ~3800 cal yr B.P., and is followed by decreases to -27.2‰ (50 cm) and -28.6‰ (0 cm) that respectively correspond to ~3800 cal yr B.P. and the present. A similar pattern of variations was found at PC-F, also of site 1. From 390 to 180 cm,  $\delta^{13}\text{C}$  varies from -27.2‰ to -26.1‰ (mean of -26.7‰).

Between 180 and 70 cm, values vary from -27.5‰ to -24.4‰ (mean of -26.3‰), and from 70 cm to 0 cm,  $\delta^{13}\text{C}$  is -27.5‰ (at 60–50 cm) and -29.0‰ at (10–0 cm) (mean of -27.7‰).  $\delta^{13}\text{C}$  values in both records from rainforest site 1 are indicative of  $\text{C}_3$  plant organic matter and do not indicate significant vegetation changes since at least ~7859 cal yr B.P. (Fig. 8A).

At sites 2 (TG) and 3 (C-CAM), the respective  $\delta^{13}\text{C}$  values of ~-17.2‰ and of ~-18.2‰ in their shallow soil layers reflect the modern vegetation cover that contains a mixture of  $\text{C}_3$  and  $\text{C}_4$  plants. The result indicates  $\text{C}_4$  plant biomass dominance of ~70% at the TG site and of ~63% at C-CAM. In order to verify the  $^{14}\text{C}$  dating of soil organic matter for these two sites, we refer to the results of more than 20  $^{14}\text{C}$  humin datings obtained in similar soils and depths at other sites in Brazil (Pessenda et al., 1998b; Freitas et al., 2001; Pessenda et al., 2001). For instance, the  $^{14}\text{C}$  soil data base suggests ~16,000 cal yr B.P. at ~270 cm soil depth, ~9000 cal yr B.P. at ~180 cm soil depth, and ~3000 cal yr B.P. at ~50–40 cm. For the deeper soil layer, the  $\delta^{13}\text{C}$  value of ~-26.0‰ suggests the dominance of  $\text{C}_3$  plants, probably mostly comprised of trees. After that, a  $\delta^{13}\text{C}$  increase to -16‰ occurs from ~180 cm (~9000 cal yr B.P.) to ~30 cm (~3000 cal yr B.P.), followed by a small decrease to ~-17.2‰ in the shallow soil layer (30–0 cm), indicating the opening of vegetation probably associated with a drier or less humid period than the previous one. A similar pattern was observed at C-CAM, where the  $\delta^{13}\text{C}$  increase occurs from ~-21.0‰ at ~140 cm, where it is interrupted by the concrectionary lateritic level, to ~-18.0‰ in the shallow soil layer (Fig. 8B).

Comparison of the  $\delta^{13}\text{C}$  values of soil samples in relation to depth and depositional ages in the paleochannel at locations MOC-F and MOC-TF of site 4 outside the flooded zone and CA-IM, CA-F of site 6 inside the flooded zone shows that they have similar  $\delta^{13}\text{C}$  patterns of change (Fig. 8C). The  $^{14}\text{C}$  dating indicates that since ~22,000 cal yr B.P. (350–340 cm) and ~9150 cal yr B.P. (150–140 cm) at MOC-F and ~7800 (350–140 cm) and ~6500 cal yr B.P. (150–140 cm) at CA-F, the mean carbon isotopic values of -24.8‰ (MOC-TF), -26.2‰ (MOC-F and CA-F), and -26.6‰ (CA-IM) indicate dominance of  $\text{C}_3$  plants, probably associated with the existence of active paleochannels. A general

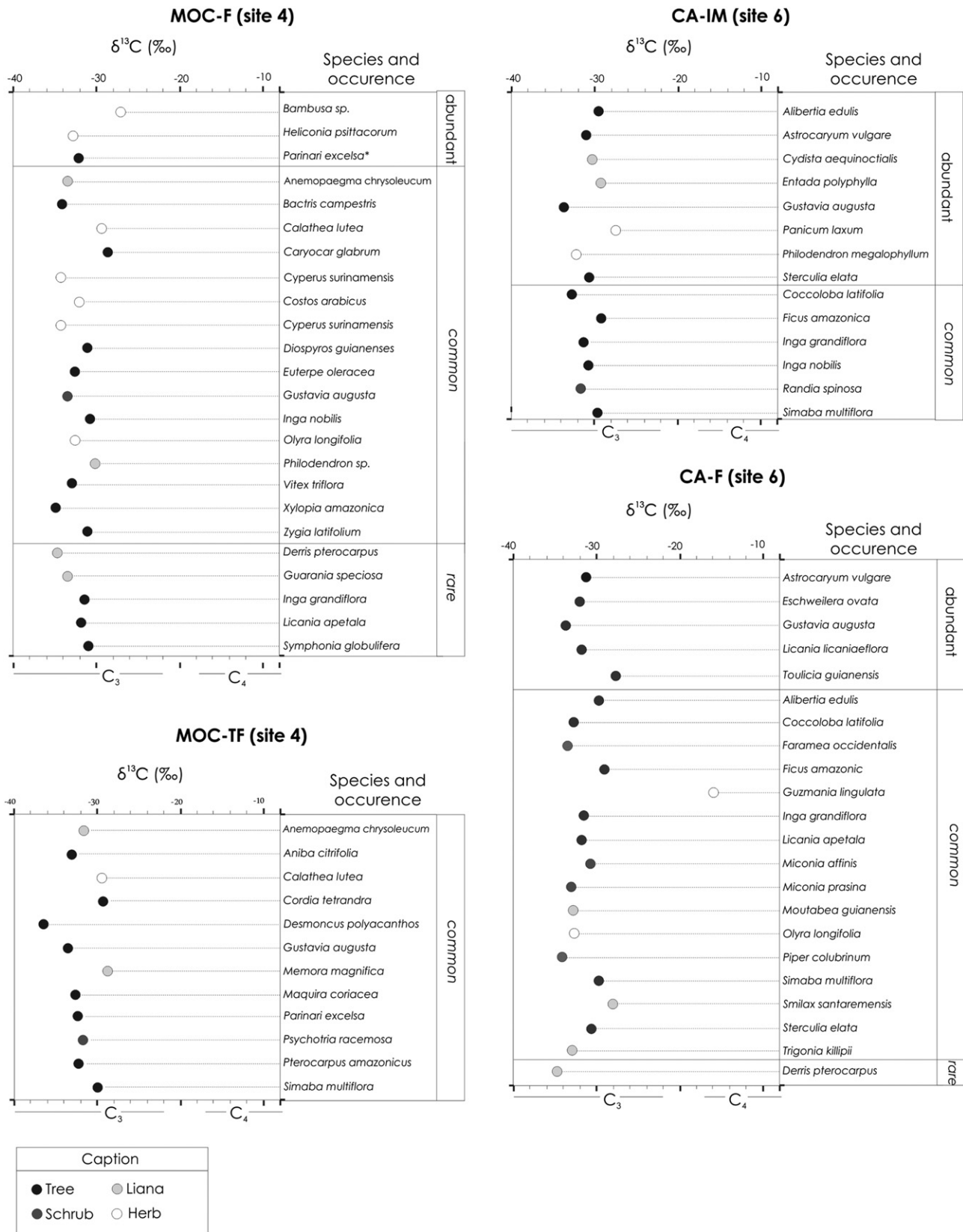


Fig. 6. Plants and their respective isotopic values ( $\delta^{13}\text{C}$ ) of forest on paleochannel site 4 (MOC-F and MOC-TF), site 6 (CA-IM and CA-F) grouped by their representativeness and vegetation habit (tree, shrub, liana and herbs).

trend towards larger  $\delta^{13}\text{C}$  values of  $-18.5\%$  at MOC-TF (70–60 cm) occurred from  $\sim 9150$  (150–140 cm) to  $\sim 2450$  cal yr B.P. (50–40 cm) at MOC-F and  $-18.8\%$  at CA-F (60–50 cm) from  $\sim 6500$  cal yr B.P.

to  $\sim 2000$  cal yr B.P., indicating the sequence of the filling of paleochannels and the establishment of a vegetation cover that was constituted of a mixture of  $\text{C}_3$  and  $\text{C}_4$  plants. From  $\sim 2450$  cal yr B.P. at MOC-F and

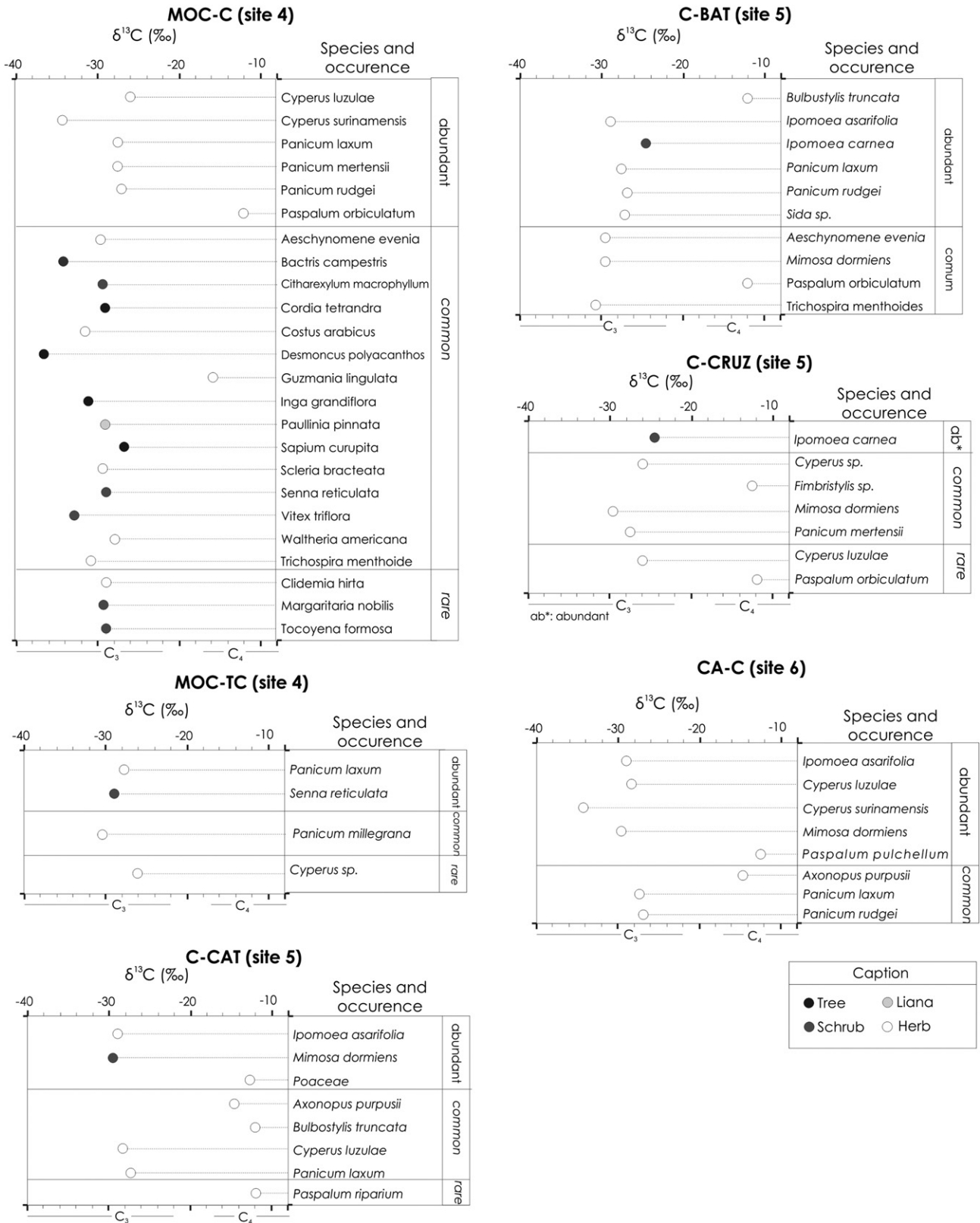
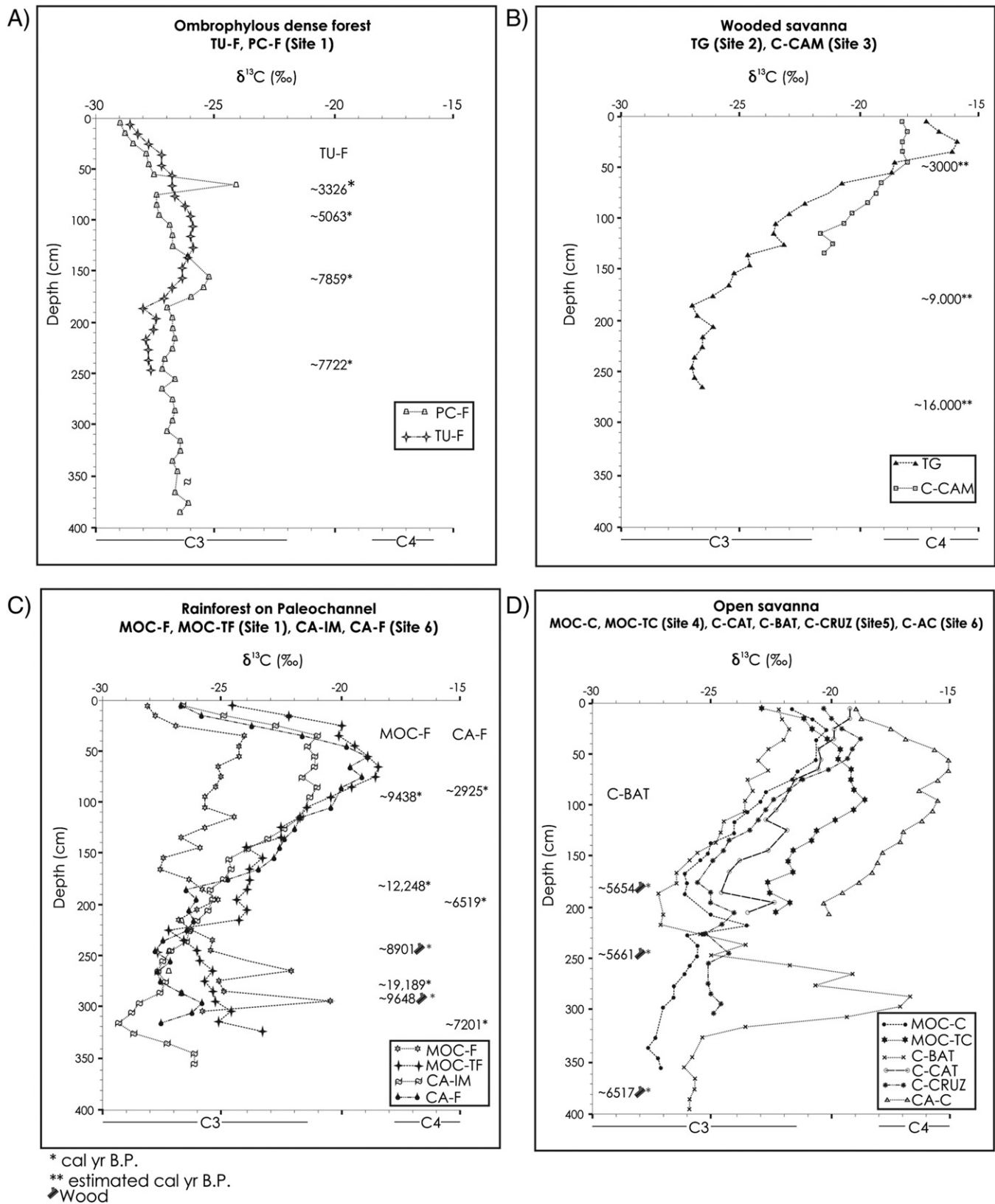


Fig. 7. Plants and their respective isotopic values ( $\delta^{13}\text{C}$ ) of open savanna site 4 (MOC-C and MOC-TC), site 5 (C-CAT, C-BAT and C-CRUZ) and site 6 (C-AC) grouped by their representativeness and stature (tree, shrub, liana and herbs).

~2000 cal yr B.P. at CA-F until the present,  $\delta^{13}\text{C}$  values became more negative, reaching between  $-20.0\text{‰}$  at MOC-TF (30–20 cm) and  $-28.1\text{‰}$  at MOC-F (10–0 cm), indicating that the paleochannels were completely filled and were covered by trees, similar to the modern environment.

The open savanna MOC-C and MOC-TC locations of site 4, both in close contact with rainforest, and the open savanna on the floodplain locations C-CAT, C-BAT, C-CRUZ of site 5 and C-AC of site 6 have similar  $\delta^{13}\text{C}$  patterns of change with soil depth (Fig. 8D). From the bottom to



**Fig. 8.** Carbon isotopic soil depth (cm) and respective ages grouped by vegetation types. (A) Forest on post-Barreiras Formation, site 1 (PC-F, TU-F); (B) Wooded savanna, site 2 (TG) and site 3 (C-CAM); (C) Forest on paleochannel, site 4 (MOC-F, MOC-TC) and site 6 (CA-IM, CA-F); (D) Open savanna, site 4 (MOC-C, MOC-TC) site 5 (C-BAT, C-CAT, C-CRUZ) and site 6 (CA-C).

~80 cm at site 4, the mean  $\delta^{13}\text{C}$  values are  $-25.1\%$  at MOC-C and  $-22.8\%$  at MOC-TC, indicating  $\text{C}_3$  plant dominances of ~86.4% and 70%, respectively. At site 5, the  $\delta^{13}\text{C}$  mean values from the bottom to ~70 cm are  $-23.1\%$  at C-BAT and C-CAT and  $-24.6\%$  at C-CRUZ,

representing  $\text{C}_3$  plant biomass contributions to the soil organic matter of ~77% at the three locations. From 70 cm to the soil surface, the values vary between  $-18.8\%$  (C-CRUZ) to  $-22.7\%$  (C-BAT) and indicate a mixture of  $\text{C}_3$  and  $\text{C}_4$  plants, with the  $\text{C}_3$  plants basically constituted by

herbs (Fig. 8D). Between ~6500 and ~5650 cal yr B.P. at C-BAT, the carbon isotope values changed sharply from ~−26.0‰ to ~−17.0‰, indicating an increase of C<sub>4</sub> plants, but possibly also associated with an eventual influence of organic matter from marine algae that typically have δ<sup>13</sup>C values of −20‰ to −22‰ (Meyers, 1994, 1997). This possibility is supported by Miranda (2010), who suggests a marine influence during the transgressive phase at locations ~13 km west of Lake Arari and ~15 km from C-BAT. A marine influence was also observed in São Luis Lake, ~80 km southeast of the sampling point from ~7000 to ~3100 cal yr B.P., based on the presence of mangrove pollen such as *Rhizophora* and *Avicennia* (França et al., 2012, in press). From ~5665 cal yr B.P. to modern, all the δ<sup>13</sup>C profiles of site 5 showed a gradually increasing pattern from ~−26.0‰ to ~−19.0‰, likely associated with a less humid/more dry period than earlier. At C-CRUZ, a slight decrease from ~−19.0‰ to ~−20.5‰ occurs at ~40 cm that is possibly associated with an increase of C<sub>3</sub> plants, as observed in the modern floristic assemblage. Isotopic values at CA-C (site 6) are the least negative when compared to the other flooding zone samples, with a mean δ<sup>13</sup>C value of ~−18.8‰ from 210 to 140 cm that is indicative of a ~59% C<sub>4</sub> plant biomass contribution. However, the C<sub>4</sub> influence becomes higher between 140 cm to the shallow soil layer, with the mean carbon isotopic value of ~−16.3‰ (Fig. 8D), which corresponds to a ~76% C<sub>4</sub> plant biomass that is reflected in the modern local dominance of Poaceae species.

#### 4.5. Past and modern environmental changes

Earlier studies done at Marajó Island have emphasized the many variables involved with environmental changes during the early to mid-Holocene, including (1) a transgressive marine phase (Cohen et al., 2005a,b; Vedel et al., 2006; França et al., in press), (2) variations in the Amazon river discharge caused by changes in rainfall in the Amazon Basin (Bush and Colinvaux, 1988; Sifeddine et al., 1994; Gouveia et al., 1997; Pessenda et al., 1998a,b; Freitas et al., 2001; Pessenda et al., 2001, 2010; Cohen et al., 2012; França et al., 2012), (3) climatic changes recorded at the same latitude, including a dry/less wet period in the late Pleistocene (Ledru et al., 2006) and early Holocene (Van der Hammen, 1974; Absy et al., 1991; Turcq et al., 1998; Freitas et al., 2001), and (4) tectonic subsidence (Rossetti et al., 2008a,b, 2012) and consequent abandonment of paleochannels (Rossetti et al., 2009).

Vegetation also changed in response to the environmental changes, and the current landscape reflects all these influences. Rainforest site 1 (TU-F, PC-F) is outside the flooding zone on the post-Barreiras Formation terrain, and it seems to have experienced less impact, inasmuch as it was not, or was at least, less affected by relative marine sea level change and tectonic subsidence. In the present setting, carbon isotope values indicate that C<sub>3</sub> plants contribute 100% of the soil organic matter, and it is possible to infer from the δ<sup>13</sup>C soil profiles that no significant vegetation changes have occurred in these places since at least ~7859 cal yr B.P.

The wooded savanna location C-CAM, which is also outside the flooding zone, carbon isotope values vary from ~−26‰ to ~−16‰ from the bottom to the shallow soil layer. This δ<sup>13</sup>C soil profile likely represents a vegetation change from C<sub>3</sub> plants (probably trees) to C<sub>4</sub> plants (grasses) associated with a less humid/dry period. Similar vegetation changes and climate inferences have been reported in other studies done at similar latitudes in northern and northeastern Brazilian regions. In the Amazon region, for example, dry periods occurred between ~9000–6000 cal yr B.P., as verified by a 250 km tropical rainforest–savanna transect (Campos of Humaitá, Fig. 1) in southern Amazonas State (Pessenda et al., 1998a; Freitas et al., 2001; Pessenda et al., 2001) and in a 400 km woody savanna (Cerrado)–tropical forest transect that included the south and north, of Rondônia State (Ariquemes, Humaitá, Pimenta Bueno, Vilhena in Fig. 1), southern Amazon region (Pessenda et al., 1998b). Both transects are located ~1700 km from the study area. In the Barreirinhas region, Maranhão

state, northeastern Brazil, ~1000 km southeast of Marajó Island, a dry/less humid period was recorded until ~6900 cal yr BP at Caço Lake (Fig. 1) in the late Pleistocene and early Holocene (Sifeddine et al., 2003; Pessenda et al., 2005; Ledru et al., 2006) and from ~10,000 to 4000 cal yr B.P. in a ~80 km vegetation transect forest (Cerrado)–woody savanna (Cerrado)–coastal forest (Restinga), in the Barreirinhas region, ~20 km from Caço Lake (Pessenda et al., 2004). At Flona, Parna and Rebio in northeastern Brazil (Fig. 1), ~2000 km from Marajó Island, soil organic matter carbon isotope values from ~18,000 cal yr B.P. to ~11,800 cal yr B.P. to ~10,000 cal yr B.P. suggest the dominance of C<sub>3</sub> arboreal vegetation associated with humid climates. The savanna expanded from ~10,000 cal yr B.P. to ~4000 cal yr B.P. during a less humid/drier climate phase as indicated by the significant presence of fires that implied by naturally buried charcoal fragments in the soil. From ~3000 cal yr B.P. to the present, soil carbon isotope records suggest forest expansion and a wetter climate phase (Pessenda et al., 2010).

The floristic characterization and carbon isotopic values indicate that vegetation on the paleochannel locations at site 4 (MOC-F, MOC-TF) and site 6 (CA-IM, CA-F) is very similar to that in the rainforest on the western side of Marajó Island at locations TU-F and PC-F of site 1. The isotopic profiles appear to be related to the channel abandonment and paleochannel development and initial covering by primary vegetation followed by establishment of rainforest (Fig. 8C). As outlined in Fig. 9, paleochannel development, structure, and the process of colonization by trees that consists of (a) the deposition of sand and silt inside channels and surrounding areas during the late Pleistocene–early Holocene, (b) a consequent decrease in water flow that led to shallowing of the channel until its eventual mid-Holocene abandonment, and (c) retention of the marginal levees that account for the slightly elevated topography of paleochannels. Flooded areas discourage rainforest, but it can colonize the higher smooth topographies of the late Holocene once the sandy bodies start to act as freshwater reservoirs and maintain the vegetation slightly higher in the landscape, a position that is responsible for protecting some areas from the effect of prolonged flooding during the rainy seasons (Rossetti et al., 2010).

The open flooded savanna sites (C-CAT, C-BAT, C-CRUZ and CA-C) probably dominate eastern Marajó Island since its surface remains submerged most of the five months of the rainy season because of the lower elevation of this side of the island due to its slight tectonic subsidence (Rossetti, 2010; Rossetti et al., 2012). The soil isotopic profiles may suggest changes in seasonality influence to which this area has been exposed (Fig. 8D). Prolonged wet periods favored the development of C<sub>3</sub> plants (trees in the paleochannels and herbs in the flooded zone) as evidenced by the values of δ<sup>13</sup>C as low as ~−26.0‰ at C-BAT (site 5). When the drier period became more significant, C<sub>4</sub> plants (herbs) were favored, and the δ<sup>13</sup>C values increased up to ~−16.0‰ (Fig. 8D). From ~5665 cal yr B.P. to modern time, a general and similar enrichment trend up to ~−15‰ occurred for all sampling points at ~50 cm soil depth, followed by generally lower values from ~−19.0‰ to ~−24‰ in the top soil layer, suggesting the return of a significantly wetter climate during the last thousand or at least few hundreds of years. It is important to notice that the wooded savanna (C-CAM) and the open flooded savanna sites have different floristic constitutions (Figs. 5 and 7); the wooded savanna is composed of distorted trees because of the high aluminum soil concentration and consists of a mixture of ~40% C<sub>3</sub> plants (mainly trees and few herbs) and ~60% C<sub>4</sub> grasses, whereas the open savanna is basically represented by C<sub>3</sub> plants (grasses and herbs) that tolerate flooded conditions.

The past vegetation reconstruction and the modern vegetation distribution allow us to estimate that future climate changes to larger seasonal and/or more variable dry/less wet period than the present can produce significant changes in the Marajó Island landscape. For example, decreased seasonality leads to less water accumulation in the modern flooding zone that will favor the expansion of C<sub>4</sub> plants in this area. Eventually, rainforest trees would be able to occupy this

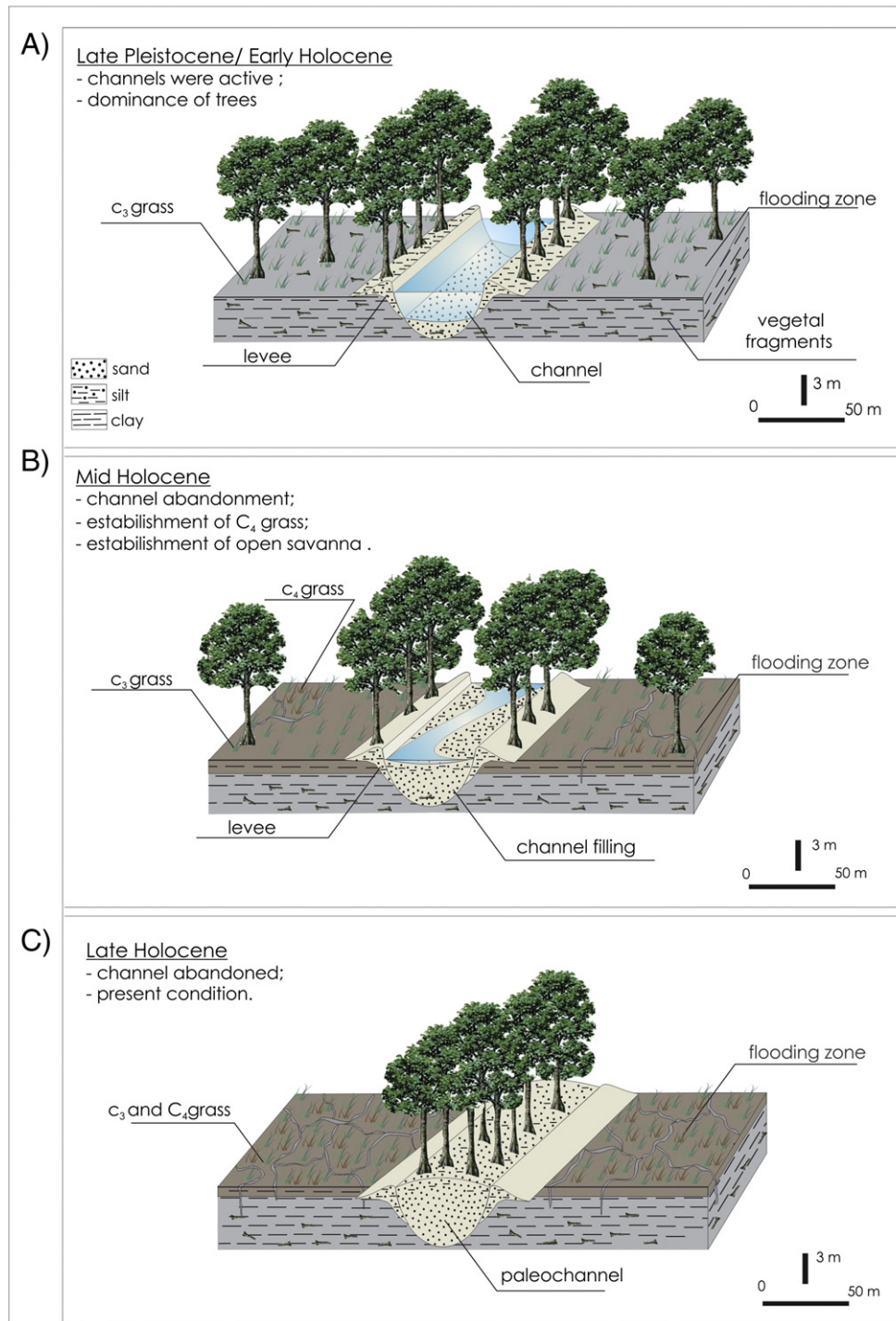


**Fig. 9.** Scheme representing the channel abandonment process during the Late Pleistocene to Late Holocene periods at northeastern section and its influence on vegetation dynamics.

place through ecological succession, thereby expanding the wooded savanna and the rainforest in the eastern part of Marajó Island.

## 5. Summary and conclusions

The distribution of flooded and non-flooded areas on Marajó Island seems to be mainly responsible for the modern distribution and the existence of the distinct phytogroups of open savanna, rainforest on post-Barreiras Formation terrain, and rainforest on paleochannels in its landscape. Non-flooded areas such as rainforest site 1 (PC-F, TU-F) and paleochannel locations (MOC-F-MOC-TF, CA-IM, CA-F), have biomass containing 93% to 100% C<sub>3</sub> plants (trees and herbs) and are very

similar in their vegetation constitutions. Wooded savanna, whose C<sub>4</sub> biomass constitution is around 63–69%, has a particular landscape similar to central-eastern Brazilian savanna. Flooded areas such as open savanna (MOC-C, MOC-TC, C-BAT, C-CAT, C-CRUZ and CA-C) contains a mixture of a few trees, C<sub>3</sub> and C<sub>4</sub> herbs, and has a C<sub>4</sub> biomass contribution ranging between 34% (C-CRUZ) and 60% (CA-C).

Climatic changes since the Late Pleistocene, which was predominantly humid, to a drier early to middle Holocene, and then a humid late Holocene, together with minor tectonic events, contributed significantly to the evolution of the past and modern vegetation mosaic forest and wooded savanna. C<sub>3</sub> plants were dominant in the south-western region of Marajó Island that is currently covered by rainforest

and wooded savanna vegetation outside the modern flooding area. From ~10,000 cal yr B.P. to ~2000 cal yr B.P., the abandonment and filling of small channels occurred, and a concurrent significant increase of C<sub>4</sub> plant biomass indicates a probable opening of vegetation that is more expressed in the flooded region and is ultimately associated with a less humid/more dry period. Since ~2000 cal yr B.P., the environment, expressed in both vegetation and climate, has been similar to present. The floristic survey integrated with carbon isotope analyses of distinct vegetation types reveals C<sub>3</sub> grass predominance in the flooded open savanna, whereas in the dry season, a mixture of C<sub>3</sub> and C<sub>4</sub> grasses occurs. In the wooded savanna, C<sub>3</sub> grasses occur less commonly, and C<sub>4</sub> grasses, although few in species, have had a more significant biomass during the dry season.

## Acknowledgments

We gratefully acknowledge the financial support of the São Paulo Foundation for Research (FAPESP), grants 2004/15518-6, 2006/52173-2, 2007/03615-5 and 2008/07330-9. We thank the two anonymous reviewers for their detailed and constructive comments that helped us improve this contribution.

## References

- Absy, M.L., Cleef, A., Fournier, M., Martin, L., Servant, M., Sifeddine, A., Ferreira Da Silva, M., Soubies, F., Suguio, K., Turcq, B., Der Hammen, Van, 1991. Th. Mise en évidence de quatre phases d'ouverture de la forêt dense dans le sud-est de l'Amazonie au cours des 60,000 dernières années. Première comparaison avec d'autres régions tropicales. *C. R. Acad. Sci.* 312 (2), 673–678.
- ANA, 2003. Hydrological Information System. Brazilian National Water Agency (On line dataset, 14.3 MB, <http://hidroweb.ana.gov.br/baixar/mapa/Bacia1.zip>).
- Arai, M., 2006. A grande elevação eustática do Mioceno e sua influência na origem do Grupo Barreiras. *Geol. USP Sér. Cient.* 6, 1–6.
- Behling, H., Costa, M.L., 2000. Holocene environmental changes from the Rio Curuá record in the Caxiuanã Region, eastern Amazon Basin. *Quat. Res.* 53, 369–377.
- Behling, H., Cohen, M.C.L., Lara, R.J., 2001. Studies on Holocene mangrove ecosystem dynamics of the Bragança Peninsula in north-eastern Pará, Brazil. *Palaeogeogr. Palaeoclimatol. Palaeoecol.* 167, 225–242.
- Bemery, R.L., 1981. Estudo sedimentológico dos paleocanais da região do Rio Paracauri, Ilha do Marajó – Estado do Pará. (Master Thesis) NCGG-UFGA, Belém (PA).
- Bezerra, P.E.L., Oliveira, W., Regis, W.D.E., Brazão, J.E.M., Gavinho, J., Coutinho, R.C.P., 1990. Amazônia legal: Zoneamento das potencialidades e dos recursos naturais. Projeto zoneamento das potencialidades dos recursos naturais da Amazônia: geologia, solos e vegetação. Instituto Brasileiro de Geografia e Estatística, Superintendência de Desenvolvimento da Amazônia, Div. 5. Rio de Janeiro, pp. 9–89.
- Boulet, R., Pessenda, L.C.R., Telles, E.C.C., Melfi, A.J., 1995. Une évaluation de la vitesse de l'accumulation superficielle de matière par la faune du sol à partir de la datation des charbons et de l'humine du sol. Exemple des latosols des versants du lac Campestre, Salitre, Minas Gerais, Brésil. *C. R. Acad. Sci.* 320 (2), 287–294.
- Boutton, T.W., 1996. Stable carbon isotope ratios of soil organic matter and their use as indicators of vegetation and climate change. In: Boutton, T.W., Yamasaki, S.I. (Eds.), *Mass Spectrometry of Soils*. Marcel Dekker, New York, pp. 47–82.
- Boutton, T.W., Archer, S.R., Midwood, A.J., Zitzer, S.F., Bol, R., 1998.  $\delta^{13}\text{C}$  values of soil organic carbon and their use in documenting vegetation change in a subtropical savanna ecosystem. *Geoderma* 82, 5–41.
- Bush, M.B., Colinvaux, P.A., 1988. A 7000-year pollen record from the Amazon lowlands, Ecuador. *Vegetatio* 76, 141–154.
- Carneiro-Filho, A., Schwartz, D., Tatumi, S.H., Rosique, T., 2002. Amazonian paleodunes provide evidence for drier climate phases during the late Pleistocene–Holocene. *Quat. Res.* 58, 205–209.
- Castro, D.F., Rossetti, D.F., Pessenda, L.C.R., 2010. Facies,  $\delta^{13}\text{C}$ ,  $\delta^{15}\text{N}$  and C/N analyses in a late Quaternary compound estuarine fill, northern Brazil and relation to sea level. *Mar. Geol.* 274, 135–150.
- Cohen, M.C.L., Souza Filho, P.W.M., Lara, R.J., Behling, H., Angulo, R.J., 2005a. A model of Holocene mangrove development and relative sea-level changes on the Bragança Peninsula (northern Brazil). *Wetl. Ecol. Manag.* 13, 433–443.
- Cohen, M.C.L., Behling, H., Lara, R.J., 2005b. Amazonian mangrove dynamics during the last millennium: the relative sea-level and the Little Ice Age. *Rev. Palaeobot. Palynol.* 136, 93–108.
- Cohen, M.C.L., Pessenda, L.C.R., Behling, H., Rossetti, D.F., França, M.C., Guimarães, J.T.F., Frias, Y.S., Smith, C.B., 2012. Holocene palaeoenvironmental history of the Amazonian mangrove belt. *Quat. Sci. Rev.* 55, 50–58.
- Cordeiro, R.C., Turcq, B., Sifeddine, A., Lacerda, L.D., Silva Filho, E.V., Gueiros, B., Potty, Y.P., Santelli, R.E., Pádua, E.O., Patchinelam, S.T., 2011. Biogeochemical indicators of environmental changes from 50 ka to 10 ka in a humid region of the Brazilian Amazon. *Palaeogeogr. Palaeoclimatol. Palaeoecol.* 299, 426–436.
- Deines, P., 1980. The isotopic composition of reduced organic carbon. In: Fritz, P., Fontes, J.C. (Eds.), *Handbook of Environmental Isotope Geochemistry. The Terrestrial Environments*, 1, pp. 329–406.
- Desjardins, T., Filho, A.C., Mariotti, A., Chauvel, A., Girardin, C., 1996. Changes of the forest–savanna boundary in Brazilian Amazonia during the Holocene as revealed by soil organic carbon isotope ratios. *Oecologia* 108, 749–756.
- França, M., Francisquini, M.I., Cohen, M.C.L., Pessenda, L.C.R., Rossetti, D.F., Guimarães, J., Smith, C.B., 2012. The last mangroves of Marajó Island–Eastern Amazon: impact of climate and/or relative sea-level changes. *Rev. Palaeobot. Palynol.* 187, 50–65.
- França, M.C., Francisquini, M.I., Cohen, M.C.L., Pessenda, L.C.R., 2014. Inter-proxy evidence for the development of the Amazonian mangroves during the Holocene. *Veg. Hist. Archaeobot.* (in press).
- Freitas, H.A., Pessenda, L.C.R., Aravena, R., Gouveia, S.E.M., Ribeiro, A.S., Boulet, R., 2001. Late Quaternary vegetation dynamics in the Southern Amazon Basin inferred from carbon isotopes in soil organic matter. *Quat. Res.* 55, 39–56.
- Gouveia, S.E.M., Pessenda, L.C.R., 2000. Datation par le C-14 de charbons inclus dans le sol pour l'étude du rôle de la remontée biologique de matière et du colluvionnement dans la formation de latosols de l'état de São Paulo, Brésil. *C. R. Acad. Sci. Paris* 330, 133–138.
- Gouveia, S.E.M., Pessenda, L.C.R., Aravena, R., Boulet, R., Roveratti, R., Gomes, B.M., 1997. Dinâmica das vegetações durante o Quaternário recente no sul do Amazonas indicada pelos isótopos do carbono (12C, 13C, 14C) do solo. *Geochim. Bras.* 11 (3), 355–367.
- Gouveia, S.E.M., Pessenda, L.C.R., Aravena, R., Boulet, R., Scheel-Ybert, R., Bendassoli, J.A., Ribeiro, A.S., Freitas, H.A., 2002. Carbon isotopes in charcoal and soils in studies of palaeovegetation and climate changes during the late Pleistocene and the Holocene in the southeast and centerwest regions of Brazil. *Glob. Planet. Chang.* 33, 95–106.
- IDESP, 1974. Estudos integrados da Ilha do Marajó. Relatório (Belém-PA).
- Kiehl, E.J., 1979. Manual de edafologia; relações solo/planta. Ceres, São Paulo.
- Ledru, M.-P., Ceccantini, G., Gouveia, S.E.M., López-Sáez, J.A., Pessenda, L.C.R., Riberito, A.S., 2006. Millennial-scale climatic and vegetation changes in a northern Cerrado (North-east, Brazil) since the last glacial maximum. *Quat. Sci. Rev.* 25, 1110–1126.
- Ledru, M.-P., Salatino, M.L.F., Ceccantini, G.T., Salatino, A., Pinheiro, F., Pintaud, J.-C., 2007. Regional assessment of the impact of climatic change on the distribution of a tropical conifer in the lowlands South America. *Divers. Distrib.* 13, 761–771.
- Lima, C.M., 2008. Dinâmica da vegetação e inferências climáticas no Quaternário Tardio na região da Ilha de Marajó (PA), empregando os isótopos do carbono (12C, 13C, 14C) da matéria orgânica de solos e sedimentos. Master Thesis, USP, Piracicaba (SP), Brazil (<http://www.teses.usp.br/teses/disponiveis/64/64134/tde-15042009-104930/pt-br.php>).
- Meyers, P.A., 1994. Preservation of elemental and isotopic source identification of sedimentary organic matter. *Chem. Geol.* 114, 289–302 (Amsterdam).
- Meyers, P.A., 1997. Organic geochemical proxies of paleoceanographic, paleolimnologic and paleoclimatic process. *Org. Geochem.* 27, 213–250.
- Miranda, M.C.C., 2010. Sedimentologia, isótopos estáveis e palinologia de depósitos quaternários no leste da Ilha do Marajó, Estado do Pará. (PhD Thesis) Instituto de Geociências, Universidade de São Paulo, São Paulo.
- Miranda, M.C.C., Rossetti, D.F., Pessenda, L.C.R., 2009. Quaternary paleoenvironments and relative sea-level changes in Marajó Island (Northern Brazil): Facies,  $\delta^{13}\text{C}$ ,  $\delta^{15}\text{N}$  and C/N. *Palaeogeogr. Palaeoclimatol. Palaeoecol.* 282, 19–31.
- Munsell, Color, 2009. Munsell Soil Color Charts, New Revised edition. Macbeth Division of Kollmorgen Instruments, New Windsor, NY.
- Pessenda, L.C.R., Valencia, E.P.E., Camargo, P.B., Telles, E.C.C., Martinelli, L.A., Cerri, C.C., Aravena, R., Rozanki, K., 1996a. Natural radiocarbon measurements in Brazilian soils developed on basic rocks. *Radiocarbon* 38, 203–208.
- Pessenda, L.C.R., Aravena, R., Melfi, A.J., Telles, E.C.C., Boulet, R., Valencia, E.P.E., Tomazello, M., 1996b. The use of carbon isotopes (C-13, C-14) in soil to evaluate vegetation changes during the Holocene in Central Brazil. *Radiocarbon* 38 (2), 191–201.
- Pessenda, L.C.R., Gomes, B.M., Aravena, R., Ribeiro, A.S., Boulet, R., Gouveia, S.E.M., 1998a. The carbon isotope record in soils along a forest–cerrado ecosystem transect: implications for vegetation changes in the Rondonia State, southwestern Brazilian Amazon region. *The Holocene* 8, 599–603.
- Pessenda, L.C.R., Gouveia, S.E.M., Aravena, R., Gomes, B.M., Boulet, R., Ribeiro, A.S., 1998b. 14C dating and stable carbon isotopes of soil organic matter in forest savanna boundary areas in the southern Brazilian Amazon region. *Radiocarbon* 40, 1013–1022.
- Pessenda, L.C.R., Boulet, R., Aravena, R., Rosolen, V., Gouveia, S.E.M., Ribeiro, A.S., Lamotte, M., 2001. Origin and dynamics of soil organic matter and vegetation changes during the Holocene in a Forest savanna transition zone, Brazilian Amazon region. *The Holocene* 11 (2), 250–254.
- Pessenda, L.C.R., Ribeiro, A.S., Gouveia, S.E.M., Aravena, R., Boulet, R., Bendassoli, J.A., 2004. Vegetation dynamics during the late Pleistocene in the Barreirinhas region, Maranhão State, northeastern Brazil, based on carbon isotopes in soil organic matter. *Quat. Res.* 62, 183–193.
- Pessenda, L.C.R., Ledru, M.P., Gouveia, S.E.M., Aravena, R., Ribeiro, A.S., Bendassoli, J.A., Boulet, R., 2005. Holocene palaeoenvironmental reconstruction in northeastern Brazil inferred from pollen, charcoal and carbon isotope records. *The Holocene* 15, 812–820.
- Pessenda, L.C.R., De Oliveira, P.E., Mofatto, M., Medeiros, V.B., Garcia, R.J.F., Aravena, R., Bendassoli, J.A., Leite, A.Z., Saad, A.R., Etchebehere, M.L., 2009. The evolution of a tropical rainforest/grassland mosaic in southeastern Brazil since 28,000 <sup>14</sup>C yr BP based on carbon isotopes and pollen records. *Quat. Res.* 71, 437–452.
- Pessenda, L.C.R., Gouveia, S.E.M., Ribeiro, A.S., De Oliveira, P.E., Aravena, R., 2010. Late Pleistocene and Holocene vegetation changes in northeastern Brazil determined from carbon isotopes and charcoal records in soils. *Palaeogeogr. Palaeoclimatol. Palaeoecol.* 297, 597–608.

- Pessenda, L.C.R., Vidotto, E., De Oliveira, P.E., Buso-Junior, A.A., Cohen, M.C.L., Ricard-Branco, F.L., Bendassolli, J.A., 2012. Late Quaternary vegetation and coastal environmental changes at Ilha do Cardoso mangrove, southeastern Brazil. *Palaeogeogr. Palaeoclimatol. Palaeoecol.* 363–364, 57–68.
- Pires, J.M., Prance, G.T., 1985. The vegetation types of the Brazilian Amazon. In: Prance, G.T., Lovejoy, T.E. (Eds.), *Key Environments: Amazonia*. Pergamon, Oxford.
- Projeto Radam, 1974. Folha SA. 22. Departamento Nacional de Produção Mineral, Belém, Rio de Janeiro.
- Reimer, P.J., Baillie, M.G.L., Bard, E., Bayliss, A., Beck, J.W., Blackwell, P.G., Bronk Ramsey, C., Buck, C.E., Burr, G.S., Edwards, R.L., Friedrich, M., Grootes, P.M., Guilderson, T.P., Hajdas, I., Heaton, T.J., Hogg, A.G., Hughen, K.A., Kaiser, K.F., Kromer, B., McCormac, F.G., Manning, S.W., Reimer, R.W., Richards, D.A., Southon, J.R., Talamo, S., Turney, C.S.M., Van der Plicht, J., Weyhenmeyer, C.E., 2009. IntCal09 and Marine09 radiocarbon age calibration curves, 0–50,000 years cal BP. *Radiocarbon* 51, 1111–1150.
- Rossetti, D.F., 2010. Tectonic control on the stratigraphy framework of late Pleistocene and Holocene deposits in Marajó Island, state of Pará, Eastern Amazonia. *An. Acad. Bras. Cienc.* 82, 439–450.
- Rossetti, D.F., Valeriano, M.M., 2007. Evolution of the lowest amazon basin modeled from the integration of geological and SRTM topographic data. *Catena* 70, 253–265.
- Rossetti, D.F., Valeriano, M.M., Goes, A.M., Thales, M., 2008a. Palaeodrainage on Marajó Island, northern Brazil, in relation to Holocene relative sea-level dynamics. *The Holocene* 18, 01–12.
- Rossetti, D.F., Góes, A.M., Valeriano, M.M., Miranda, A.C.C., 2008b. Quaternary tectonics in a passive margin: Marajó Island, northern Brazil. *J. Quat. Sci.* 23, 121–135.
- Rossetti, D.F., Góes, A.M., Toledo, P.M., 2009. Archeological Mounds in Marajó Island in northern Brazil: a geological perspective integrating remote sensing and sedimentology. *Geoarchaeology* 24 (1), 22–41.
- Rossetti, D.F., Almeida, S., Amaral, D.D., Lima, C.M., Pessenda, L.C.R., 2010. Coexistence of forest and savanna in an Amazonian area from a geological perspective. *J. Veg. Sci.* 21, 120–132.
- Rossetti, D.F., Souza, L.S.B., Prado, R., Elis, V.R., 2012. Neotectonics in the northern equatorial Brazilian margin. *J. S. Am. Earth Sci.* 37, 175–190.
- Sifeddine, A., Fröhlich, F., Fournier, M., Martin, L., Servant, M., Soubiès, F., Turcq, B., Suguio, K., Volkmer-Ribeiro, C., 1994. La sédimentation lacustre indicateur de changements des paléoenvironnements au cours des 30.000 dernières années (Carajás, Amazonie, Brésil). *Geosci. Surf.* 1645–1652.
- Sifeddine, A., Marint, L., Turcq, B., Volkmer-Ribeiro, C., Soubiès, F., Cordeiro, R.C., Suguio, K., 2001. Variations of the Amazonian rainforest environment: a sedimentological record covering 30,000 years. *Palaeogeogr. Palaeoclimatol. Palaeoecol.* 168, 221–235.
- Sifeddine, A., Albuquerque, A.L.S., Ledru, M.P., Turcq, B., Knoppers, B., Martin, L., Mello, W.Z., Passenau, H., Dominguez, J.M.L., Cordeiro, R.C., Abrão, J.J., Bitterncourt, A.C.S.P., 2003. A 21,000 cal years paleoclimatic record from Caçó Lake, northern Brazil: evidence from sedimentary and pollen analyses. *Palaeogeogr. Palaeoclimatol. Palaeoecol.* 189, 25–34.
- Soil Survey Staff, 1999. United States Department of Agriculture, Soil taxonomy: a basic system of soil classification for making and interpreting soil surveys Second edition. *Agriculture Handbook*, 436. USDA, Washington.
- Turcq, B., Sifeddine, A., Martin, L., Absy, M.L., Soubies, F., Suguio, K., Volkmer-Ribeiro, C., 1998. Amazonia rainforest fires: a lacustrine record of 7,000 years. *Royal Swedish Academy of Sciences. Ambio* 27 (2), 139–142.
- Van der Hammen, T., 1974. The Pleistocene changes of vegetation and climate in tropical South America. *J. Biogeogr.* 1, 3–26.
- Vedel, V., Behling, H., Cohen, M.C.L., Lara, R.J., 2006. Holocene mangrove dynamics and sea-level changes in northern Brazil, inferences from the Taperebal core in northeastern Pará State. *Veg. Hist. Archaeobot.* 15, 115–123.
- Vidotto, E., Pessenda, L.C.R., Ribeiro, A.S., Freitas, H.A., Bendassolli, J.A., 2007. Dinâmica do ecótono floresta-campo no sul do estado do Amazonas no Holoceno através de estudos isotópicos e fitossociológicos. *Acta Amazon.* 37, 389–404.
- Zani, H., Rossetti, D.F., Cohen, M.L.C., Pessenda, L.C.R., Cremon, E.H., 2012. Influence of landscape evolution on the distribution of floristic patterns in northern Amazonia revealed by  $\delta^{13}\text{C}$  data. *J. Quat. Sci.* 27 (8), 854–864.